



Since January 2020 Elsevier has created a COVID-19 resource centre with free information in English and Mandarin on the novel coronavirus COVID-19. The COVID-19 resource centre is hosted on Elsevier Connect, the company's public news and information website.

Elsevier hereby grants permission to make all its COVID-19-related research that is available on the COVID-19 resource centre - including this research content - immediately available in PubMed Central and other publicly funded repositories, such as the WHO COVID database with rights for unrestricted research re-use and analyses in any form or by any means with acknowledgement of the original source. These permissions are granted for free by Elsevier for as long as the COVID-19 resource centre remains active.



Temporal dynamics, diversity, and interplay in three components of the virodiversity of a Mallard population: Influenza A virus, avian paramyxovirus and avian coronavirus



Michelle Wille^a, Alexis Avril^{a,b}, Conny Tolf^a, Anna Schager^a, Sara Larsson^a, Olivia Borg^a, Björn Olsen^{c,d}, Jonas Waldenström^{a,*}

^a Centre for Ecology and Evolution in Microbial Model Systems, Linnaeus University, SE-391 82 Kalmar, Sweden

^b CIRAD, Campus international de Baillarguet, 34398 Montpellier, France

^c Section of Infectious Diseases, Department of Medical Sciences, Uppsala University, SE-751 85 Uppsala, Sweden

^d Zoonosis Science Centre, Department of Medical Biochemistry and Microbiology, Uppsala University, SE-751 85 Uppsala, Sweden

ARTICLE INFO

Article history:

Received 14 August 2014

Received in revised form 23 October 2014

Accepted 14 November 2014

Available online 21 November 2014

Keywords:

Avian paramyxovirus

Co-infection

Coronavirus

Disease dynamics

Influenza A virus

Newcastle disease virus

ABSTRACT

Multiple infections, or simultaneous infection of a host with multiple parasites, are the rule rather than the exception. Interactions between co-occurring pathogens in a population may be mutualistic, competitive or facilitative. For some pathogen combinations, these interrelated effects will have epidemiological consequences; however this is as yet poorly incorporated into practical disease ecology. For example, screening of Mallards for influenza A viruses (IAV) have repeatedly revealed high prevalence and large subtype diversity in the Northern Hemisphere. Other studies have identified avian paramyxovirus type 1 (APMV-1) and coronaviruses (CoVs) in Mallards, but without making inferences on the larger viral assemblage. In this study we followed 144 wild Mallards across an autumn season in a natural stopover site and constructed infection histories of IAV, APMV-1 and CoV. There was a high prevalence of IAV, comprising of 27 subtype combinations, while APMV-1 had a comparatively low prevalence (with a peak of 2%) and limited strain variation, similar to previous findings. Avian CoVs were common, with prevalence up to 12%, and sequence analysis identified different putative genetic lineages. An investigation of the dynamics of co-infections revealed a synergistic effect between CoV and IAV, whereby CoV prevalence was higher given that the birds were co-infected with IAV. There were no interactive effects between IAV and APMV-1. Disease dynamics are the result of an interplay between parasites, host immune responses, and resources; and is imperative that we begin to include all factors to better understand infectious disease risk.

© 2014 Elsevier B.V. All rights reserved.

1. Introduction

Viruses, particularly RNA viruses, are the most abundant parasites of humans, animals and plants (Domingo, 2010). Despite this assertion, there is only limited information on fundamental aspects of RNA virus ecology and epidemiology. For instance, with the exception of humans and Indian Flying Foxes (*Pteropus giganteus*; Anthony et al., 2013), we know very little about viral diversity in animals, and the effects they have on their hosts. RNA viral abundance and diversity can be attributed to large population sizes, short generation times, and high mutation and recombination rates (Domingo, 2010; Elena et al., 2000). Within a single virus group there are a number of subdivisions to consider, including

different subtypes, which compete for the same resources, and the distribution of closely related variants that make up the viral population (quasispecies), which may confer a fitness advantage to one of these subtypes (Arbiza et al., 2010; Miralles et al., 2001; Ojosnegros et al., 2011). However, it is multiple infections, or the simultaneous infections with multiple parasite species in an individual host, rather than independent infections that is the rule rather than the exception (Bordes and Morand, 2011; Woolhouse, 2002). Yet, investigations on the impacts of multiple infections on individual host or host populations are still scarce in disease ecology (Bordes and Morand, 2011). Most surveillance schemes provide information on a single pathogen, in a population of animals, in a snapshot of time. Hence it is difficult to assess patterns and dynamics of infection of a single pathogen, let alone an assemblage of pathogens. Although it is well established that members of different virus families can utilize the same host, the

* Corresponding author.

E-mail address: jonas.waldenstrom@lnu.se (J. Waldenström).

dynamics of possible interdependent influences between different viruses in their natural host, including inhibition and facilitation, is still unknown. Infections with viruses belonging to different taxa can occur as co-infections, where two or more different viruses infect the host at the same time, or where the second virus infects the host at a later time point, referred to as superinfection. Alternatively, dynamics can be dominated by sequential infections, where the initial infection has been cleared before the host is infected by the same or a different virus. If co-infections are occurring in individuals or the population of hosts, the effects may range from synergistic interactions, whereby one virus might enhance the other, to antagonistic interactions, whereby one virus may inhibit the other (Carrillo et al., 2007; Elena et al., 2000; Elena and Sanjuan, 2005; Moya et al., 2000). This is driven by competition for resources, such as receptors or cells, or immune modulation, such as immune suppression or the result of cross immunity (Bordes and Morand, 2011; Miralles et al., 2001). Thus co-infection and sequential infections may be a driver in disease dynamics.

Avian viruses are best described in poultry species due to the economic implications of disease for the industry. Less is known about RNA viruses in wild birds, despite the role that migratory birds play as reservoirs for several avian specific pathogens and zoonoses (Chan et al., 2013; Thomas et al., 2007). Wild birds have been implicated in the introduction of pathogens into poultry, in addition to acting as carriers following spill over from poultry into wild birds (Alexander, 2007; Cha et al., 2013; Jorgensen et al., 2004). Furthermore, many species are migratory, and thus have the propensity to move pathogens long distances (Altizer et al., 2011; Bauer and Hoye, 2014). The Mallard (*Anas platyrhynchos*) is a model species for bird-borne infections as it straddles the interface between wild birds and the domestic bird industry. It is the most abundant and wide-spread duck in the world due to an adaptability to a wide range of habitats, and its tolerance of human presence and disturbance (Cramp and Simmons, 1977; Drilling et al., 2002). It acts as a reservoir for some viruses, especially influenza A viruses (IAV), and has been found to play a role in the epidemiology of several other RNA viruses such as avian paramyxovirus type 1 (APMV-1), and coronaviruses (CoV) (Latorre-Margalef et al., 2014; Muradrasoli et al., 2009; Tolf et al., 2013b). While these viruses are unrelated, they occur in apparently healthy migrating ducks.

We have previously screened for IAV, APMV-1 and CoV in migratory Mallards at a stopover site in SE Sweden (Latorre-Margalef et al., 2014). At this site, IAV peaks in the Mallard population in the autumn months with rates up to 30% and as many as 74 different HA/NA combinations have been detected (Latorre-Margalef et al., 2014). APMV-1 has been detected in the late autumn, at very low prevalence (2%) (Tolf et al., 2013a), whereas CoV has been detected at high prevalence in the context of the evaluation of a screening method (Muradrasoli et al., 2009) at this study site. In this study we follow 144 Mallards across the autumn of 2011 and evaluate the prevalence and patterns of IAV, APMV-1 and CoV to further characterize the natural history of these viruses at our study site. Further, we infer patterns and dynamics of co-infections to determine whether there is dependence, competition, or co-existence in the wild Mallard host. This is the first study following three RNA viruses across a season in a group of birds to examine prevalence rates and genotype/subtype distributions, and to investigate relationships between different viruses in an important host species.

2. Methods

2.1. Sample collection

Wild Mallards were captured in a duck trap situated at Ottenby Bird Observatory, Sweden (56° 12'N, 16° 24'E) as part of a

long-term IAV sampling scheme. Upon first capture, all individuals are weighed, measured and ringed with a unique numbered metal ring. At each capture, either the cloaca was swabbed, or freshly deposited faeces were collected from the bottom of a single-use cardboard box. Samples were placed in virus transport media (VTM) and stored at -70°C within 2–6 h of collection. Detailed capture and sampling methods at our study site have been previously described (Latorre-Margalef et al., 2014). For the purpose of this study, we wanted to follow a group of 144 birds that utilized the area over an autumn season. This group reflected a number of age groups (73 juveniles, 60 adults, 11 unknown age), sexes (57 females, 86 males, 1 unknown), and arrival dates across the season. The number of sampling occasions ranged from 1 to 71 per individual, where 12.7% of individuals were only sampled once, and 62% of individuals were sampled on more than 10 occasions. Ethical approval for trapping and sampling was obtained from the Swedish Animal Research Ethics Board (“Linköpings djurförsöksetiskanämnd”, reference numbers 46-09 and 111-12).

2.2. Sample screening

Viral RNA was extracted from VTM containing samples with the MagNA Pure 96™ Nucleic Acid Purification System (Roche, Mannheim, Germany) and MagNA Pure 96 DNA and Viral Nucleic Acid Large Volume Kit (Roche) following manufacturer's recommendations. VTM samples were diluted 1:4 with PBS prior to extraction. Following extraction, samples were assayed by real time reverse transcriptase PCR (rRT-PCR) for IAV, APMV-1, and CoV using previously published methods. Briefly, IAV was screened using a rRT-PCR assay targeting a short region of the matrix gene (Spackman et al., 2002) and APMV-1 was assayed using a rRT-PCR targeting the matrix (M) gene (Tolf et al., 2013b; Wise et al., 2004) with the One Step RT-PCR Kit (Qiagen, Hilden, Germany). A pan-coronavirus rRT-PCR assay targeting the RNA-dependant RNA polymerase (RdRp) gene (Muradrasoli et al., 2009) and the iScript One Step RT-PCR Kit (BioRad, Hercules, USA) was used for CoV. A threshold cut off (Ct) of 40 was used for all rRT-PCR screens.

2.3. Virus characterization

All samples positive for IAV, and samples positive for APMV-1 that were IAV negative with C_t -values below 35 were propagated in 10–11 day old embryonated chicken eggs (Valo, Germany). Eggs were inoculated via the allantoic route, and allantoic fluid was harvested two days following inoculation. The fluid was assayed for the presence of IAV or APMV-1 using a haemagglutination assay. Samples positive for IAV were subsequently subtyped using a haemagglutination inhibition test with antisera raised in rabbits against all haemagglutinin (HA) subtypes. RNA was extracted from allantoic fluid using the High Pure RNA Isolation Kit following manufacturer's specifications (Roche) and the neuraminidase (NA) subtype was determined using a number of available PCR assays (Wille et al., 2013).

The near complete F-gene of the APMV-1 virus was amplified using the ONE Step RT-PCR Kit (Qiagen) and NDV + 47Fw and NDV + 1671Rev primers (Tolf et al., 2013b) following RNA extraction, resulting in a 1599 bp amplicon. The reaction contained 5× Buffer, 2.5 mM of additional MgCl_2 , 0.2 mM of each dNTP, 0.5 mM of each primer, 6 units RNasin (Promega), 0.8 μl Enzyme Mix, 2 μl RNA, and water to a final volume of 20 μl . Thermocycling conditions were 50 $^{\circ}\text{C}$ for 30 min, 95 $^{\circ}\text{C}$ for 15 min, followed by 45 cycles of 95 $^{\circ}\text{C}$ for 30 s, 55 $^{\circ}\text{C}$ for 20 s, 60 $^{\circ}\text{C}$ for 5 min, followed by a final extension at 60 $^{\circ}\text{C}$ for 7 min. The PCR products were cleaned using the Wizard® SV Gel and PCR Clean-Up System (Promega, Madison, USA) and cloned using the pGEM-T Cloning Vector System (Promega) according to manufacturer's instructions. Three to

five clones from each PCR product were sequenced with the T7 and SP6 primers at Macrogen Inc. (Amsterdam, The Netherlands).

A nested PCR approach was utilized to amplify a segment of the RdRp gene of CoV (Chu et al., 2011) from original material. Viruses with Ct-values below 35 were selected. The first PCR was completed using the ONE Step RT-PCR Kit (Qiagen), wherein the reaction contained 5× Buffer, 2.5 mM of additional MgCl₂, 0.2 mM of each dNTP, 0.5 mM of each primer, 6 units RNAsin (Promega), 1 μl Enzyme Mix, 2 μl RNA, and water to a final volume of 25 μl. Thermocycling conditions were 50 °C for 30 min, 95 °C for 15 min, followed by 40 cycles of 95 °C for 30 s, 48 °C for 20 s, 60 °C for 5 min, followed by a final extension at 60 °C for 7 min. The PCR product was diluted 1:1000, and then amplified with a second set of primers using Taq Polymerase (Qiagen). The reaction contained 10× Buffer, 1.5 mM MgCl₂, 0.2 mM of each dNTP, 0.5 mM of each primer, 0.5 units Taq polymerase, 2 μl PCR product, and water to a final volume of 25 μl. Thermocycling conditions were 94 °C for 10 min, followed by 40 cycles of 94 °C for 20 s, 48 °C for 30 s, 72 °C for 50 s, followed by a final extension at 72 °C for 7 min. PCR products were purified using the Wizard[®] SV Gel and PCR Clean-Up System (Promega) and sequenced at Eurofins MWG Operon (Ebersberg, Germany). APMV-1 or CoV sequences were aligned using the MAFFT algorithm (Katoh et al., 2009) within Geneious R6 (Biomatters, New Zealand). Phylogenetic models were determined in MEGA 5.2 (Tamura et al., 2011), and Maximum Likelihood Trees were built using Garli 2.0 (Zwickl, 2006) and bootstrapped 1000 times. All sequences generated in this study have been deposited in GenBank under the accession numbers KM015306–KM015347 (Tables A.1 and A.2).

2.4. Trends in virus prevalence and interactions

Seasonal prevalence for each of the three viruses were estimated using Generalized Linear Mixed Models (GLMMs) with a logit link function to account for binomial responses (presence/absence of infection in a given individual at a given capture occasion). Samples were collected from Julian day 216 to 347 (4 August–31 December 2011), but only days 250 (7 September) to 347 were used due to few capture occasions, translating to high uncertainty in the temporal trend, prior to this period. The seasonal trends were modeled as polynomial functions of the Julian day. The best order polynomial was evaluated through Akaike information criterion (AIC) (Bolker et al., 2009; Burnham and Anderson, 2002), Pearson's statistics, and residual plots (McCullagh and Nelder, 1989) (Tables A.3–A.5). We investigated whether the seasonal risk of infection was modulated by co-infection with another virus by adding a binary covariate factor describing co-infection for each capture occasion. We only considered the influence of IAV infection on the seasonal prevalence of CoV and APMV-1 starting from the total interaction models $\text{logit}(\text{CoV}) = \text{IAV} * \text{season}$ and $\text{logit}(\text{APMV1}) = \text{IAV} * \text{season}$ (Tables A.4 and A.5). The influence of CoV on APMV-1 infection, or vice versa, and the influence of CoV or APMV-1 on IAV were not investigated because of low prevalence rates for these viruses, hence poor explanatory power. Models were fitted with lme4 package (Bates, 2005) for R software (R Development Core Team, 2008).

Seasonal variation in IAV subtype proportions were estimated with Vector Generalized Linear Models (VGLMs) implemented in VGAM package (Yee, 2010) and allowing for modeling multinomial responses (details given in (Latorre-Margalef et al., 2014)). Based on the evolutionary history of the HA, the different subtypes were divided into HA Clades, whereby the H1 Clade includes H1, H2, H5, H6, the H3 Clade includes H3, H4, and the H11 Clade includes H11. Rare viruses, such as H8, H9, H10, and H12 were not included due to only few observations in the dataset. The seasonal trend was modeled using polynomial regressions on 5 day intervals. As we

only used the models to describe prevalence rather than to draw inferences, we did not include random effects, which also reduced computational issues. Isolates prior to Julian day 285 (12 October) were not included as there were only four isolates (across 49 days) prior to this day.

3. Results

3.1. Seasonal variation in prevalence of viruses

IAV, APMV-1, and CoV exhibited different seasonal prevalence patterns at the population level. Of 3029 samples collected, 574 were positive for IAV (18.9%), 56 for APMV-1 (1.8%) and 208 for CoV (6.9%). Temporally, IAV prevalence was lower during the early autumn and 2 peaks occurred between Julian day 290 and 330 (mid-October to mid-November), with each peak at almost 30% (Fig. 1A); a pattern consistent with previous observations at this study site (Latorre-Margalef et al., 2014). The first peak observed at day 260 is based on fewer than 20 samples per day and only 10 positive individuals (Fig. A.1), resulting in large confidence intervals on estimates, and therefore will not be further discussed. These 574 positive samples were collected from 111 individuals, which were infected at 1–14 trapping occasions. Of the non-infected birds, 50% were sampled on only one occasion (Fig. A.1). APMV-1 was rare at the study site, with a total of 17 detections prior to Julian day 315, followed by an increase in prevalence, peaking at 2% on day 330 (Fig. 1A). The 56 APMV-1 positive samples were collected from 34 individuals. Infections were detected in most birds only once, but infections were detected three times in eight individuals and four times in two individuals (Fig. A.1). Temporally, the pattern of CoV was similar to IAV, with two peaks of prevalence, an initial peak of ~12% and a secondary peak of ~9% (Fig. 1A). As with IAV, the peak at day 250 is based on few samples and positive individuals resulting in very large confidence intervals. The first peak occurred at Julian day 285, and coincided with immigration of ducks (Fig. A.1), and the second peak coincided with the peak of APMV-1. The 208 CoVs were detected in 75 different individuals and there was large heterogeneity of infections, where a few individuals accounted for the majority of the infection positive days, particularly during the first prevalence peak (Fig. A.1).

3.2. Co-infections, individual infection histories, and virus co-existence

Overlapping seasonal prevalence curves of the three pathogens illustrated the circulation of multiple viruses at the same time in the population. Furthermore, IAV and CoV co-circulated in the population at high prevalence (>25% and >9% respectively) on two occasions (Fig. 1B), corresponding to a large influx of birds to the study site (Fig. A.1), and co-circulation of all three viruses starting on Julian day 315 (Fig. 1A). The occurrence of co-infection within individuals followed the expected pattern based on the prevalence of viruses at the site; a high level of individual co-infections when more than one virus had a high prevalence (Fig. 1). Of the 62 detected co-infection events, all but two included IAV. The largest number of co-infections occurred between IAV and CoV, and the number of co-infection days was the highest during the first and second CoV prevalence peaks. Polynomial models revealed a slight increasing risk of being infected by CoV when infected by IAV (models $\text{logit}(\text{CoV}) = \text{IAV} + \text{season}$, (IAV effect estimate on the risk of CoV infection: 0.28 ± 0.18 ; $df = 1$; $p = 0.13$)). However, models with and without IAV as explanatory variable showed equal support to the data ($\text{logit}(\text{CoV}) = \text{IAV} + \text{season}$ vs $\text{logit}(\text{CoV}) = \text{season}$, AIC = 1424.221 vs 1424.441, respectively) (Table A.5 and Fig. 2). Regardless of the polynomial degree used for the seasonal trend,

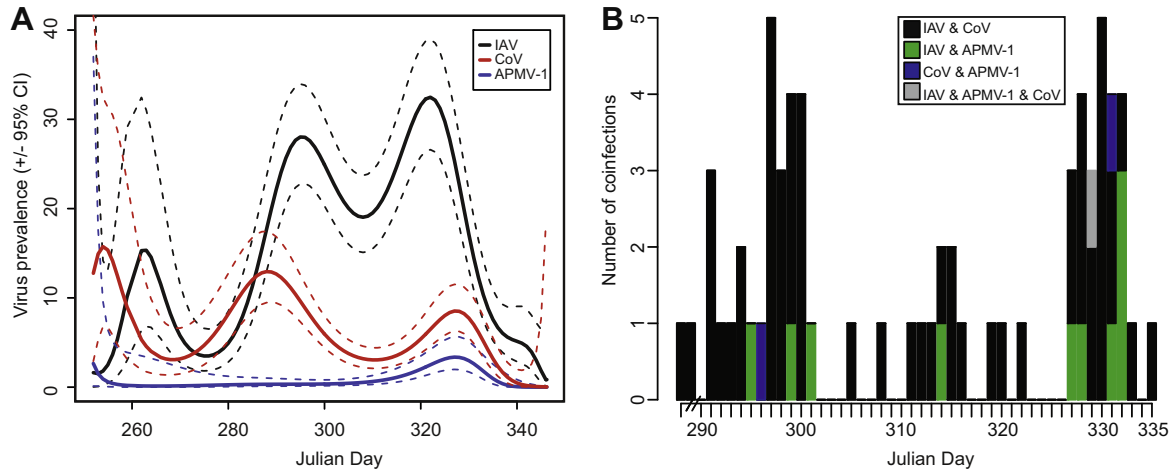


Fig. 1. Prevalence of three viruses in 144 Mallards followed over time at Ottenby in 2011. (A) Population prevalence of each virus (solid lines) with 95% confidence intervals (dashed lines) for days the Julian days 250–347. Model selection parameters are presented in Tables A.3–A.5. (B) Number of co-infection events, plotted from Julian day 290 to 335. There were 2 co-infection events prior to day 290.

all models including IAV effects had similar, or better support than the corresponding models without IAV as a covariate (Table A.5). Similarly, the highest number of co-infections with APMV-1 occurred when the prevalence of this virus peaked. However, we could not find any statistical support for a synergistic effect between APMV-1 and IAV (models $\text{logit}(\text{APMV-1}) = \text{IAV} + \text{season}$ vs $\text{logit}(\text{APMV-1}) = \text{IAV}$, AIC = 495.44 vs 495.33); but 1 model showed a negative effect of IAV (Table A.4 and Fig. A.3). Despite the rarity of this virus at the study site prior to Julian day 315, there were a number of APMV-1 co-infection days prior to this day (5 co-infections in 17 detections). A co-infection event including all three viruses occurred on only a single occasion, Julian day 329, when all the viruses were circulating in the population (Fig. 1B).

At an individual level, 26 birds had no detectable virus, however most of these individuals were only sampled on a few occasions (mean number of samples = 3.6). Forty individuals (27.8%) were infected only with one virus, 34 of which were positive for only IAV, and 78 (54%) were infected with more than one virus at the time of capture during the study period. Of these individuals, 40 birds had sequential infections only (the bird was infected with more than one virus, but never on the same day) as inferred from our sampling regime (mean number of samples = 32, SD = 16.3) and the remaining 38 individuals exhibited co-infections (infection

with more than one virus on the same day) and sequential infections (mean number of samples = 30.5, SD = 16.8). A single individual was co-infected without the detection of a sequential infection, however only two samples were collected from this individual. In the subset of birds that were co-infected ($n = 38$), co-infections occurred on average 1.7 days, representing 28% of infection positive days (Fig. A.4). Despite IAV not being involved in all co-infection events, of the birds infected with more than one virus, all individuals were infected or co-infected with IAV at some point during the sampling regime (Fig. A.5). More juvenile, or first year, birds were co-infected ($\chi^2 = 8.879$, $df = 2$, $p = 0.0118$), but there was no difference in the age class when considering sequential and co-infections together ($\chi^2 = 5.724$, $p = 0.0572$). There was no effect of sex on either co-infections only ($p = 0.46$), or co- and sequential infections ($p = 1$).

Given the subset of individuals infected with IAV, approximately two thirds of these individuals were infected with more than one virus, and a third exhibited co-infection. In contrast, individuals that were positive for APMV-1 ($n = 32$) and CoV ($n = 70$) were almost all infected with more than one virus. Co-infections occurred in 41% and 49% of individuals that were positive for APMV-1 and CoV, respectively; the remaining individuals only exhibited sequential infections and on rare instances, infections by only one of the viruses. (Fig. A.5). Seventeen individuals were infected with all three viruses, however only six of these exhibited days of co-infection (35%), where co-infections were predominantly between CoV and IAV (mean number of samples collected = 39) (Fig. A.5).

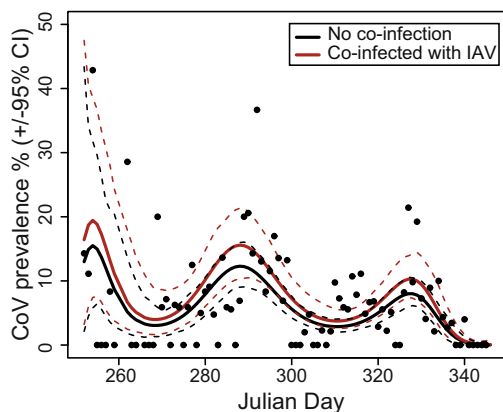


Fig. 2. A synergistic effect on avian coronavirus (CoV) prevalence when accounting for influenza A virus (IAV) infection in the population. Daily estimates of CoV prevalence are plotted as points. Model selection parameters for the curves are presented in Table A.5.

3.3. Characterization of IAV, APMV-1, and CoV

From 547 IAV positive samples, 177 were successfully propagated (32% isolation success). Eleven different HA subtypes were found, corresponding to 27 HA/NA subtype combinations. The most common subtype found was H4N6 (37), followed by H3N8 (25), H11N9 (17), H3N2 (12) and H6N2 (12) (Table A.6). Overall, the largest proportion of viruses were from the H3 Clade (H3, H4) (Fig. 3B) due to the across season presence of H3 and the large number H4 viruses detected starting on Julian day 305 (Fig. 3B). Viruses in the H1 Clade (H1, H2, H5, H6) had a higher proportion of occurrence towards the start (H6 viruses) and end of the season (H1, H2, H5 viruses), and H11 viruses were present in low numbers across the season (Fig. 3).

Nine samples positive for APMV-1 were cultured in eggs and demonstrated agglutination activity. The F gene of seven APMV-1 isolates were successfully sequenced and BLAST analysis suggest that all APMV-1 viruses belonged to Class II, Genotype I. Pairwise comparisons showed that six of the seven viruses were within 99.9% identity, and APMV-1/Mallard/Sweden/131826/2011 was only 98.5% similar to the other viruses. This was reflected phylogenetically, as this virus did not cluster with the other sequenced viruses (Fig. 4). Further, these seven viruses were between 98.5% and 99.2% similar to viruses isolated and sequenced from our study site in 2010 (Accession KC631386–95). In addition to very high sequence similarity, these isolates had the same F0 protein cleavage site sequence ¹¹²GKQGR*^{L117}, which suggest that none of the isolates were of a velogenic pathotype (Table A.1). Phylogenetic analysis provided evidence for common ancestry (of viruses isolated in mallards at Ottenby) with viruses detected in Africa and Eurasia, and more distant relationships with those isolated from birds sampled in North America and the Far East (Fig. 4).

A region of the RNA-dependant RNA polymerase (RdRp) of 35 gamma CoVs were amplified and sequenced, contributing the largest number of sequences from a single wild bird species and location to date. Phylogenetic analysis demonstrated that all viruses sequenced were gammaCoVs. Overall, the sequences were closely related to those from waterfowl in Hong Kong (Chu et al., 2011). Despite low phylogenetic resolution within the avian gammaCoV (due to short branch lengths, polytomies, and low bootstrap support), pairwise distances indicated two main groups of sequences with 95–97% similarity in our dataset. These two clusters contained sequences from viruses isolated during both the first and second peak of prevalence, suggesting the co-circulation of viruses with more than one genetic RdRp lineage (Fig. 5). Additionally,

there were 2 sequences for CoV from Mallards in our study, which did not cluster into the two main groups, and these were 96% (Avian CoV/Anas platyrhynchos/90A74286/133583/22.11.11/Sweden), and 96–98% (Avian CoV/Anas platyrhynchos/90A88528/131643/24.10.11/Sweden) similar to the other main clades (Fig. 5 and Table A.2).

More than one CoV positive sample from 9 individuals were sequenced to try to capture the change in genetic variability over time. However, from these serially sampled individuals, there was no clear pattern of RdRp lineage turn-over (Table A.7). There was a change in phylogenetic placement of samples collected 3 days apart, compared with no change in phylogenetic placement of three samples collected from an individual 13 and 61 days apart (Table A.7).

4. Discussion

Due to their proximity to urbanized areas and being permissive to domestication, Mallards are found at the interface between wildlife, poultry and humans. Further, due to large population sizes and their role in food production, Mallards constitute the largest pool of susceptible aquatic bird hosts, making this species an important model and sentinel species for avian disease research (Cramp and Simmons, 1977; Drilling et al., 2002). Mallards have been an important feature for IAV research, and at our study site have been sampled since 2002 (Latorre-Margalef et al., 2014). Patterns of prevalence, subtype, and sequence information demonstrate that IAV and APMV-1 circulating in the Mallard population in 2011 are similar to those from previous years (Latorre-Margalef et al., 2014; Tolf et al., 2013b), and in the case of APMV-1, similar to patterns found in other locations in Europe (Lindh et al., 2008; Snoeck et al., 2013), and globally (Ramey et al., 2013). This is one of six investigations including CoV in wild birds (Chu et al., 2011; Hughes et al., 2009; Jonassen et al., 2005; Muradrasoli et al., 2010, 2009; Woo et al., 2009), but the first to include temporal patterns and serially sampled individuals for these viruses. Indeed, we know very little about the actual biology of these viruses, but we predict that they exhibit similar etiology to Turkey CoV due to the detection in faeces and cloacal swabs: putative replication in intestinal epithelial cells and the epithelium of the bursa of Fabricius (Guy, 2000). Unlike other CoV from avian origins, such as IBV and Turkey CoV which exhibit clinical signs, the clinically asymptomatic nature of the lineage of CoV included in this study (Fig. 5) [avian CoV], mean that they have only been recently detected, and there is much of the ecology and epidemiology that remains to be clarified.

Although different parasites often infect and co-exist within the same host, the effects of multiple and sequential infections are only beginning to be understood. Co-infections were rare overall, as on average, birds only had 1.7 co-infection days, and not all individuals had detected co-infection days. Rather, we detected sequential infections with occasional co-infections interspersed. Despite a limited number of co-infections events, there was a synergistic effect when birds infected with CoV were also infected with IAV. On the contrary, there was no effect between APMV-1 and IAV. IAV and APMV-1 have been co-detected in wild bird samples, but the relationship between these two viruses remains unclear (e.g. Jindal et al., 2009; Lindh et al., 2008; Tolf et al., 2013b). IAV and APMV-1 utilize the α 2,3 sialic acid receptors on host cells, and may compete for host cell machinery during viral replication (Markwell, 1991). In lab studies, it has been demonstrated that there are limited synergistic or competition effects between IAV and APMV-1, but thus far studies have failed to provide a conclusive picture of the interactions at the host level (Franca et al., 2014; Ge et al., 2012; Tolf et al., 2013b). Regardless

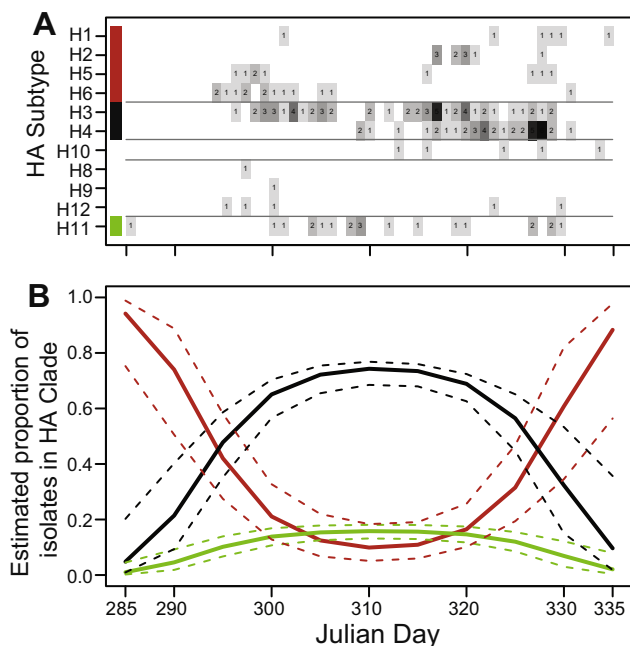


Fig. 3. Distribution of influenza A virus haemagglutinin (HA) subtypes with time. (A) Total number of isolates of each subtype per day. (B) Estimated proportion of each three HA clades isolated from the study site, calculated at 5-day intervals. Solid lines depict the mean prediction and dotted lines the 95% confidence interval of the predictions. The H1 Clade is depicted in red and includes H1, H2, H5, and H6. The H3 Clade is depicted in black and includes H3 and H4. The H11 Clade is depicted in green. Other HA subtypes and clades were not modeled due to a low number of total isolates. There are four isolates prior to this period (Julian Day 285–336), which were not included. (For interpretation of the references to color in this figure legend, the reader is referred to the web version of this article.)

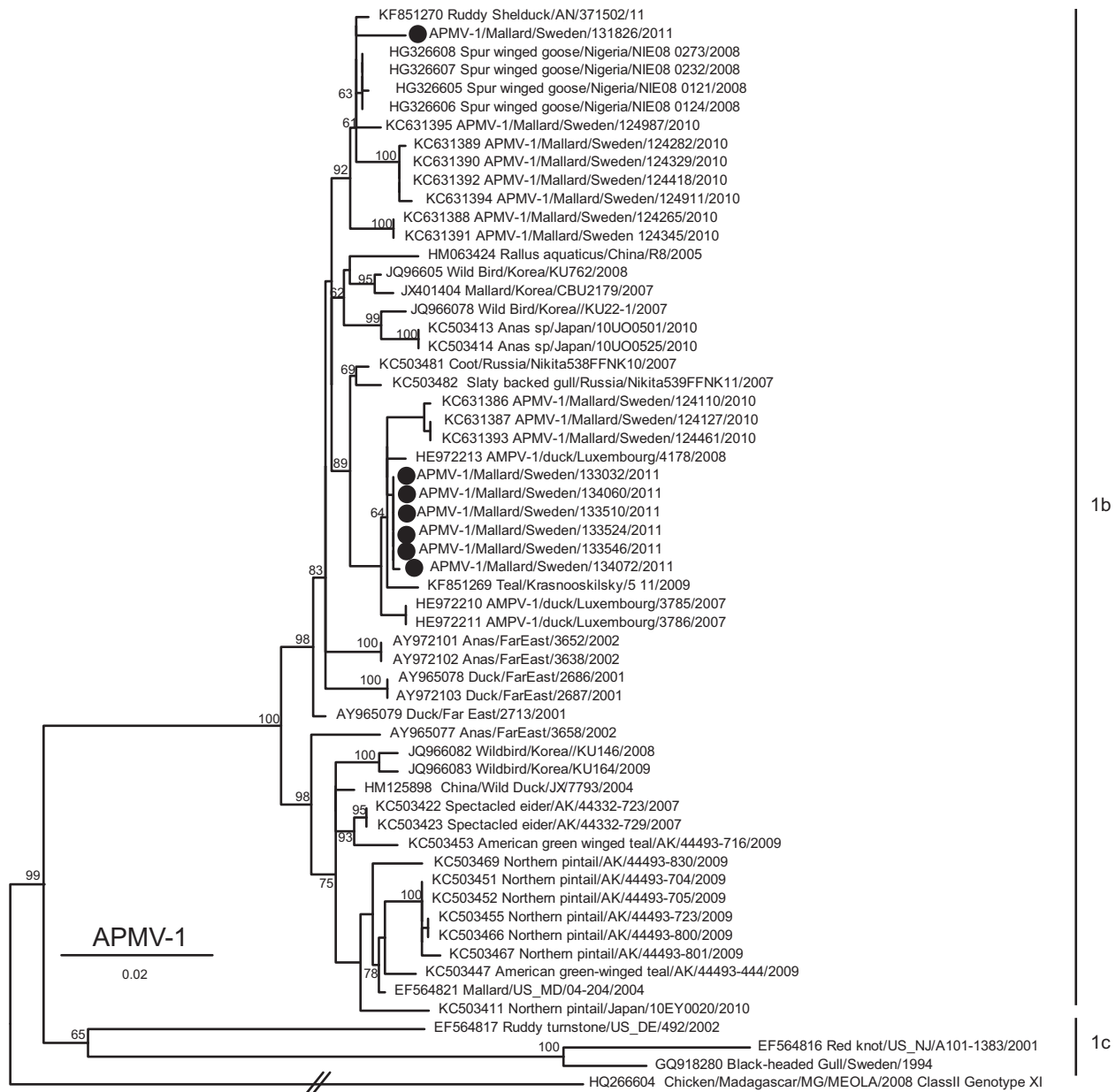


Fig. 4. Maximum likelihood tree of the F-gene of the class II genotype I Avian Paramyxovirus-1. Sub-genotype 1b and 1c are indicated and the Class II Genotype XI isolate HQ266604 was used as an outgroup. Viruses generated in this study are indicated in black circles. The scale bar indicates the number of substitutions per site.

of other variables, IAV is a major component in the wild Mallard system, as all but 2 co-infections included IAV. Therefore, all other viruses must be able to co-exist, or compete with IAV, and multiple subtypes of IAV. The co-existence of these viruses utilizing a similar niche (both at the species level, but also putatively at cell type level) may reflect long-term adaptation of these viruses to limit competition in a shared host, and highlights the need for additional laboratory studies investigating the interactions of viruses within their hosts. Further, the clinically asymptomatic nature of these viral infections suggests the host has a high carrying capacity for viral infections, making it an interesting system to pursue the topic of infection tolerance or resistance (Boots, 2008).

The host can be viewed as an ecosystem, or a landscape, for the viruses that infect it. However, this ecosystem is not static. There is an arms-race between pathogens developing better mechanisms to escape immune pressure, and hosts developing better arms in which to clear infectious agents (Clarke et al., 1994). Hence it is

important to consider both interactions between viruses, and interactions between viruses and hosts. Viruses modulate the host immune response in order to be successful; following infection of host cells, the NS1 protein of IAV is responsible for anti-interferon (IFN) activities (Garcia-Sastre, 2011; Hale et al., 2008). One could hypothesize that this may be exploited by CoVs resulting in the observed synergistic effect. Despite this viral modulation, Mallards mount a strong innate immune response to IAV, which enable them to clear IAV infections in days. In addition, an adaptive immune response follows which reduces both homosubtypic and heterosubtypic re-infection, which they maintain throughout the autumn, winter and early spring (Barber et al., 2008; Latorre-Margalef et al., 2013; Tolf et al., 2013a; Vandervan et al., 2012). Therefore, at the very least, other infecting viruses need to tolerate the mounted immune response against IAV, particularly the innate response. The predicted immune responses of the ducks could possibly explain the double peak of IAV and CoV, which is not

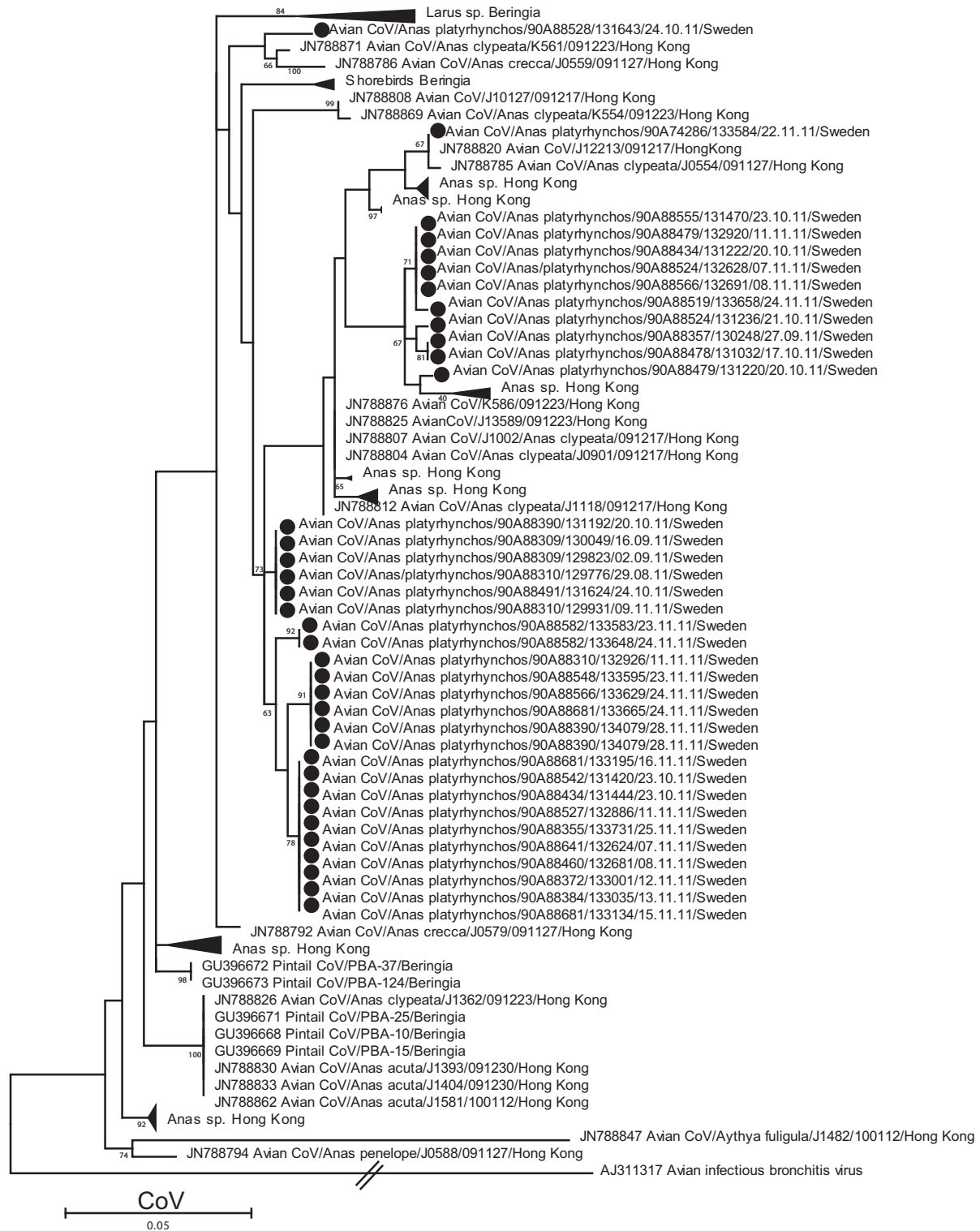


Fig. 5. Maximum likelihood tree of the partial RNA-dependant RNA polymerase of gammacoronaviruses. Infectious Bronchitis Virus is set as an outgroup. Viruses generated in this study are indicated in black circles. Naming scheme for viruses collected in Sweden are Host Species/Ring Number/Sample Number/Day.Month.Year/Location. The scale bar indicates the number of substitutions per site.

explained by virus competition: the population may have developed herd immunity against the viruses in peak A, and a virus which has been able to escape the adaptive immune response could have been introduced and proliferated during peak B. This could further have been amplified by an influx of immunologically naïve ducks to the study site directly prior to, and during, the

second prevalence peak. This is demonstrated by a turnover of different HA subtypes and Clades across the season. However, from sequencing of the CoV RdRp gene from the same individuals, there are no clear patterns of virus lineage turnover, but this could be confounded by recombination (Lai, 1996; Woo et al., 2009). Furthermore, this gene is not under direct pressure from the immune

system, so it is not an ideal candidate to investigate viral turn over in this context. Finally, temporally, the highest number of APMV-1 infections occurred when duck innate immunity is presumably the highest. An inspection of the infection histories of APMV-1 positive birds suggests these individuals have been at the study site for some time (average 29 days) prior to having an APMV-1 infection, and that this virus was circulating at the study site prior to the prevalence peak towards the end of the season. Thus, one hypothesis is that the host population was not at an optimal immune state. Alternatively, it could be due to a specific interaction with the parasitic, bacterial or viral assemblage we have not investigated. In addition to the collection and characterization of viruses within hosts, the characterization of the host immune state (from blood samples) could provide better evidence for the above hypotheses, and be a major factor in explaining viral dynamics (e.g. Tolf et al., 2013a).

Metagenomic analysis has revolutionized the study of bacterial communities, ranging from ocean water, to soil, to the digestive tracts of humans and animals (Xu, 2006), including a duck species (Strong et al., 2013). Temporally structured studies reveal changes in community composition, likely resulting from resource availability and competition. Viral metagenomics is certainly the way of the future, but to date studies are extremely limited, both in overall number and host species investigated (Bibby, 2013). Indeed, using viral metagenomics Anthony et al. (2013) predicted 32,000 viruses are to be discovered in mammals. The single viral metagenomic study in birds – domestic Turkey gastrointestinal tract, revealed numerous members of the Picornaviridae, Leviviridae, Caliciviridae and novel RNA virus sequences (in addition to DNA viruses, bacteria, fungi and eukaryotes) (Day et al., 2010). Co-infection greatly affects virus fitness, in addition to the capacity of the host to mitigate infection. Where our virus catalogue is meagre, we are limited to interactions between hosts and a small number of viruses. However, there is growing evidence that incorporating more realistic levels of parasite and pathogen diversity into epidemiological research is essential for managing infectious disease risk (Johnson et al., 2013).

Acknowledgements

We want to thank F. Johnsson and S. Andersson for assistance in sample collection, A. Jawad for assistance in virus isolation, and S. Muradrasoli and J. Eliasson for advice in setting up the CoV rRT-PCR. This work was supported by the Swedish Research Councils VR (2010-3067, 2010-5399, 2011-3568), FORMAS (2009-1220), and the EC FP6 program NewFlubird. MW was supported by a PGS-D2 fellowship from the Natural Science and Engineering Research Council of Canada. The funding sources had no role in study design, collection, analysis, interpretation of data, writing of the report, or in the decision to submit the paper for publication. This is publication No. 284 from Ottenby Bird Observatory.

Appendix A. Supplementary data

Supplementary data associated with this article can be found, in the online version, at <http://dx.doi.org/10.1016/j.meegid.2014.11.014>.

References

Alexander, D.J., 2007. An overview of the epidemiology of avian influenza. *Vaccine* 25, 5637–5644.
 Altizer, S. et al., 2011. Animal migration and infectious disease risk. *Science* 331, 296–302.
 Anthony, S.J. et al., 2013. A strategy to estimate unknown viral diversity in mammals. *mBio* 4, e00598–00513. <http://dx.doi.org/10.1128/mBio.00598-13>.

Arbiza, J. et al., 2010. Viral quasispecies profiles as the result of the interplay of competition cooperation. *BMC Evol. Biol.* 10.
 Barber, M.R.W. et al., 2008. Association of RIG-I with innate immunity of ducks to influenza. *Proc. Natl. Acad. Sci. U.S.A.* 107, 5913–5918.
 Bates, D.M., 2005. Fitting linear mixed models in R Using the lme4 package. *R News* 5, 27–30.
 Bauer, S., Hoyer, B.J., 2014. Migratory animals couple biodiversity and ecosystem functioning worldwide. *Science* 344, 54. <http://dx.doi.org/10.1126/Science.1242552>.
 Bibby, K., 2013. Metagenomic identification of viral pathogens. *Trends Biotechnol.* 31, 275–279.
 Bolker, B.M. et al., 2009. Generalized linear mixed models: a practical guide for ecology and evolution. *Trends Ecol. Evol.* 24, 127–135.
 Boots, M., 2008. Fight or learn to live with the consequences? *Trends Ecol. Evol.* 23, 248–250.
 Bordes, F., Morand, S., 2011. The impact of multiple infections on wild animal hosts: a review. *Infect. Ecol. Epidemiol.* 1. <http://dx.doi.org/10.3402/iee.v3401i3400.7346>.
 Burnham, K.P., Anderson, D.R., 2002. Model selection and multimodel inference: a practical information-theoretic approach. Springer.
 Carrillo, F.Y.E. et al., 2007. The effect of co- and superinfection on the adaptive dynamics of vesicular stomatitis virus. *Infect. Genet. Evol.* 7, 69–73.
 Cha, R.M. et al., 2013. The pathogenicity of avian metapneumovirus subtype C wild bird isolates in domestic turkeys. *Virol. J.* 10, 38. <http://dx.doi.org/10.1186/1743-1422X-1110-1138>.
 Chan, J.F. et al., 2013. Interspecies transmission and emergence of novel viruses: lessons from bats and birds. *Trends Microbiol.* 21, 544–555.
 Chu, D.K. et al., 2011. Avian coronavirus in wild aquatic birds. *J. Virol.* 85, 12815–12820.
 Clarke, D.K. et al., 1994. The red queen reigns in the kingdom of RNA viruses. *Proc. Natl. Acad. Sci. U.S.A.* 91, 4821–4824.
 Cramp, S., Simmons, K.E.L., 1977. Mallard (*Anas platyrhynchos*). In: Cramp, S., Simmons, K.E.L., Ferguson-Lees, I.J., Gillmor, R., Hollom, P.A.D., Hudson, R., Nicholson, E.M., Ogilvie, M.A., Olney, P.J.S., Voous, K.H., Wattle, J. (Eds.), *Birds of the Western Palearctic*. Oxford University Press, London, pp. 505–519.
 Day, J.M. et al., 2010. Metagenomic analysis of the turkey gut RNA virus community. *Virol. J.* 7, 313.
 Domingo, E., 2010. Mechanisms of viral emergence. *Vet. Res.* 41, 38–51.
 Drilling, N. et al., 2002. Mallard (*Anas platyrhynchos*). In: Poole, A. (Ed.), *Birds of North America Online*. Cornell Lab of Ornithology, Ithaca, <http://bna.birds.cornell.edu/bna/species/658>.
 Elena, S.F., Sanjuan, R., 2005. RNA viruses as complex adaptive systems. *Biosystems* 81, 31–41.
 Elena, S.F. et al., 2000. The two faces of mutation: extinction and adaptation in RNA viruses. *IUBMB Life* 49, 5–9.
 Franca, M. et al., 2014. Co-infection of mallards with low-virulence Newcastle disease virus and low-pathogenic avian influenza virus. *Avian Pathol.* 43, 96–104.
 Garcia-Sastre, A., 2011. Induction and evasion of type I interferon responses by influenza viruses. *Virus Res.* 162, 12–18.
 Ge, S. et al., 2012. Evaluating viral interference between Influenza virus and Newcastle disease virus using real-time reverse transcription-polymerase chain reaction in chicken eggs. *Virol. J.* 9, 128. <http://dx.doi.org/10.1186/1743-422X-9-128>.
 Guy, J.S., 2000. Turkey coronavirus is more closely related to avian infectious bronchitis virus than to mammalian coronaviruses: a review. *Avian Pathol.* 29, 207–212.
 Hale, B.G. et al., 2008. The multifunctional NS1 protein of influenza A viruses. *J. Gen. Virol.* 89, 2359–2376.
 Hughes, L.A. et al., 2009. Genetically diverse coronaviruses in wild bird populations of northern England. *Emerg. Infect. Dis.* 15, 1091–1094.
 Jindal, N. et al., 2009. Phylogenetic analysis of Newcastle disease viruses isolated from waterfowl in the upper midwest region of the United States. *Virol. J.* 6, 191.
 Johnson, P.T. et al., 2013. Host and parasite diversity jointly control disease risk in complex communities. *Proc. Natl. Acad. Sci. U.S.A.* 110, 16916–16921.
 Jonassen, C.M. et al., 2005. Molecular identification and characterization of novel coronaviruses infecting graylag geese (*Anser anser*), feral pigeons (*Columba livia*) and mallards (*Anas platyrhynchos*). *J. Gen. Virol.* 86, 1597–1607.
 Jorgensen, P.H. et al., 2004. Strains of avian paramyxovirus type 1 of low pathogenicity for chickens isolated from poultry and wild birds in Denmark. *Vet. Rec.* 154, 497–500.
 Katoh, K. et al., 2009. Multiple alignment of DNA sequences with MAFFT. *Methods Mol. Biol.* 537, 39–64.
 Lai, M.M.C., 1996. Recombination in large RNA viruses: coronaviruses. *Semin. Virol.* 7, 381–388.
 Latorre-Margalef, N. et al., 2013. Heterosubtypic immunity to influenza A virus infections in Mallards may explain existence of multiple virus subtypes. *PLoS Pathog.* 9 (6), e1003443. <http://dx.doi.org/10.1371/journal.ppat.1003443>.
 Latorre-Margalef, N. et al., 2014. Long-term variation in influenza A virus prevalence and subtype diversity in a migratory Mallards in northern Europe. *Proc. R. Soc. B* 281 (20140098), 2014. <http://dx.doi.org/10.1098/rspb.2014.0098>.
 Lindh, E. et al., 2008. Orthomyxo-, paramyxo- and flavivirus infections in wild waterfowl in Finland. *Virol. J.* 5, 35. <http://dx.doi.org/10.1186/1743-1422X-1185-1135>.

- Markwell, M.A.K., 1991. New frontiers opened by the exploration of host cell receptors. In: Kingsbury, D.W. (Ed.), *The Paramyxoviruses*, first ed. Plenum, London, pp. 407–425.
- McCullagh, P., Nelder, J.A., 1989. *Generalized Linear Models*. Chapman & Hall, London, U.K.
- Miralles, R. et al., 2001. Multiple infection dynamics has pronounced effects on the fitness of RNA viruses. *J. Evol. Biol.* 14, 654–662.
- Moya, A. et al., 2000. The evolution of RNA viruses: a population genetics view. *Proc. Natl. Acad. Sci. U.S.A.* 97, 6967–6973.
- Muradrasoli, S. et al., 2009. Broadly targeted multiprobe QPCR for detection of coronaviruses: coronavirus is common among mallard ducks (*Anas platyrhynchos*). *J. Virol. Methods* 159, 277–287.
- Muradrasoli, S. et al., 2010. Prevalence and phylogeny of coronaviruses in wild birds from the Bering Strait area (Beringia). *PLoS ONE* 5, e13640. <http://dx.doi.org/10.1371/journal.pone.0013640>.
- Ojosnegros, S. et al., 2011. Quasispecies as a matter of fact: viruses and beyond. *Virus Res.* 162, 203–215.
- R Development Core Team, 2008. R: a Language and Environment for Statistical Computing. R Foundation for Statistical Computing, Vienna, Austria.
- Ramey, A.M. et al., 2013. Genetic diversity and mutation of avian paramyxovirus serotype 1 (Newcastle disease virus) in wild birds and evidence for intercontinental spread. *Arch. Virol.* 158, 2495–2503.
- Snoeck, C.J. et al., 2013. Characterization of newcastle disease viruses in wild and domestic birds in Luxembourg from 2006 to 2008. *Appl. Environ. Microbiol.* 79, 639–645.
- Spackman, E. et al., 2002. Development of a Real-Time Reverse Transcriptase PCR assay for type A influenza virus and the avian H5 and H7 hemagglutinin subtypes. *J. Clin. Microbiol.* 40, 3256–3260.
- Strong, T. et al., 2013. Amplicon pyrosequencing and ion torrent sequencing of wild duck eubacterial microbiome from fecal samples reveals numerous species linked to human and animal. *F1000 Res.* 2, 224. <http://dx.doi.org/10.12688/f1000research.2-224.v2>.
- Tamura, K. et al., 2011. MEGA5: molecular evolutionary genetics analysis using maximum likelihood, evolutionary distance, and maximum parsimony methods. *Mol. Biol. Evol.* 28, 2731–2739.
- Thomas, N.J. et al., 2007. *Infectious Diseases of Wild Birds*. Blackwell Publishing, Ames, U.S.A.
- Tolf, C. et al., 2013a. Individual variation in influenza A virus infection histories and long-term immune responses in mallards. *PLoS ONE* 8, e61201. <http://dx.doi.org/10.1371/journal.pone.0061201>.
- Tolf, C. et al., 2013b. Prevalence of avian paramyxovirus type 1 in Mallards during autumn migration in the western Baltic Sea region. *Virol. J.* 10, 285. <http://dx.doi.org/10.1186/1743-422X-10-285>.
- Vandervlen, H.A. et al., 2012. Avian influenza rapidly induces antiviral genes in duck lung and intestine. *Mol. Immunol.* 51, 316–324.
- Wille, M. et al., 2013. Frequency and patterns of reassortment in natural influenza A virus infection in a reservoir host. *Virology* 443, 150–160.
- Wise, M.G. et al., 2004. RNA-dependent RNA polymerase gene analysis of worldwide Newcastle disease virus isolates representing different virulence types and their phylogenetic relationship with other members of the paramyxoviridae. *Virus Genes* 104, 71–80.
- Woo, P.C. et al., 2009. Coronavirus diversity, phylogeny and interspecies jumping. *Exp. Biol. Med.* 234, 1117–1127.
- Woolhouse, M.E.J., 2002. Population biology of emerging and re-emerging pathogens. *Trends Microbiol.* 10, S3–S7.
- Xu, J., 2006. Microbial ecology in the age of genomics and metagenomics: concepts, tools, and recent advances. *Mol. Ecol.* 15, 1713–1731.
- Yee, T.W., 2010. The VGAM package for categorical data analysis. *J. Stat. Softw.* 32, 1–34.
- Zwickl, D.J., 2006. Genetic algorithm approaches for the phylogenetic analysis of large biological sequence datasets under the maximum likelihood criterion. PhD Dissertation. The University of Texas at Austin.